DEVELOPMENTAL DYNAMICS 227:524–535, 2003

ARTICLE

Selective Control of Neuronal Cluster Size at the Forebrain/Midbrain Boundary by Signaling From the Prechordal Plate

Alexandra Tallafuß,[1,2] Birgit Adolf,[1,2] and Laure Bally-Cuif[1,2]*

Within the vertebrate embryonic neural plate, the first neuronal clusters often differentiate at the border of patterning identities. Whether the information inherent in the intersection of patterning identities alone controls all aspects of neuronal cluster development (location, identity, and size) is unknown. Here, we focus on the cluster of the medial longitudinal fascicle (nMLF) and posterior commissure (nPC), located at the forebrain/midbrain (fore/mid) boundary, to address this issue. We first identify expression of the transcription factor Six3 as a common and distinct molecular signature of nMLF and nPC neurons in zebrafish, and we use this marker to monitor mechanisms controlling the location and number of nMLF/nPC neurons. We demonstrate that *six3* expression is induced at the fore/mid boundary in *pax2.1/no-isthmus* and *smoothened/slow muscle omitted* mutants, where identities adjacent to the *six3* cluster are altered; however, in these mutants, the subpopulation of *six3*-positive cells located within the mispatterned territory is reduced. These results show that induction of the *six3* cluster is triggered by the information derived from the intersection in patterning identities alone, whereas correct cluster size depends, in a modular manner, on the identities themselves. The size of the *six3* cluster is also controlled independently of neural tube patterning: we demonstrate that the prechordal plate (PCP) is impaired in *mixer/bonnie and clyde* mutants and that this phenotype secondarily results in an increased production of *six3*-positive cells at the fore/mid boundary, without correlatively affecting patterning in this area. Thus, a signaling process originating from the PCP distinguishes between neural patterning and the control of *six3* cluster size at the fore/mid junction in vivo. Together, our results suggest that a combination of patterning-related and -unrelated mechanisms specifically controls the size of individual early neuronal clusters within the anterior neural plate. *Developmental Dynamics 227:524–535, 2003.*

Key words: medial longitudinal fascicle, MLF; posterior commissure, PC; diencephalon; mesencephalon; forebrain; midbrain; neural plate; prechordal plate; neurogenesis; boundary; Nodal; zebrafish

Received 10 January 2003; Accepted 23 April 2003

INTRODUCTION

At early developmental stages, all vertebrates display a similar and highly reproducible neuronal pattern. Two neuronal clusters are among the first focal sites of differentiation: one in the basal fore- and midbrain and the second at the base of the optic stalk. They generate the nucleus of the medial longitudinal fascicle (nMLF) and the tract of the postoptic commissure (TPOC), respectively (Wilson et al., 1990; Ross et al., 1992; Easter et al., 1993; Chédotal et al., 1995; Mastick and Easter, 1996; reviewed in Kimmel, 1993; Easter, 1994). These clusters have distinct sizes, neurotransmitter phenotypes, axonal routes, and targets. How neural tube regionalization, neurogenesis, and proliferation events are integrated to achieve this stereotypical pattern of differentiation is not fully understood.

[1]Zebrafish Neurogenetics Junior Research Group, Institute of Virology, Technical University-Munich, Munich, Germany
[2]GSF-National Research Center for Environment and Health, Institute of Developmental Genetics, Neuherberg, Germany
Grant sponsor: VolkswagenStiftung Association; Grant sponsor: DFG; Grant number: BA2024/2-1.
*Correspondence to: Laure Bally-Cuif, GSF-National Research Center for Environment and Health, Institute of Developmental Genetics, Ingolstaedter Landstrasse 1, D-85764 Neuherberg, Germany. E-mail: bally@gsf.de

DOI 10.1002/dvdy.10329

At early stages, the borders of expression of several patterning genes often reflect axonal routes (Wilson et al., 1993, 1997; Macdonald et al., 1994). Detailed expression studies and functional analyses support a direct or indirect role for some of these patterning genes in the formation or the refinement of axon trajectories (Macdonald et al., 1997; Mastick et al., 1997; Ba-Charvet et al., 1998; Bertuzzi et al., 1999; Hallonet et al., 1999; Hjorth and Key, 2001). The cues controlling the location and size of the first differentiation clusters have been comparatively less well studied. Transition zones in the regions of expression of different combinations of patterning genes also correlate with the position of the first neuronal clusters. For example, the differentiating neuron cell bodies of the MLF and the posterior commissure (nPC) overlap with the anteroposterior (AP) transition between the mesencephalon and caudal prosencephalon (later on referred to as fore/mid boundary), as defined by anatomic and molecular landmarks (Macdonald et al., 1994; Mastick and Easter, 1996). Similarly, the nMLF lies at the dorsal boundary of *shh* expression along the dorsoventral (DV) axis (Macdonald et al., 1994; Barth and Wilson, 1995). Based on these observations, it has been proposed that the stereotypical arrangement of the first neuronal clusters responds to the intersection of distinct positional identities.

Two (nonexclusive) mechanisms can account for the regulation of neuronal cluster size (Fig. 1). First, cluster size might respond to neural tube patterning, such that fewer or more neurons are produced when one of two neighboring identities is altered (Fig. 1, model 1). For instance, the perturbation of the fore/mid boundary by lack of the transcription factor Pax6, normally expressed in the prosencephalon, results in the generation of fewer PC neurons in the mouse (Mastick et al., 1997). Second, cluster size might also be controlled independently of neural tube patterning (Fig. 1, models 2a and b). Here, mechanisms might be general and affect all neuronal clusters (model 2a). An example is the lateral inhibition process mediated by Notch/Delta signaling, which regulates the number of neurons differentiating from every proneural cluster (see Lewis, 1998; Chitnis, 1999; Blader and Strähle, 2000, for reviews). Other cell-intrinsic or -extrinsic mechanisms might control the number of neurons in single clusters (model 2b). Examples of cell-intrinsic information might be the expression of neuron subtype-specific transcription factors, the absence of which affects the development of one neuronal population along AP or DV. For instance, motor neurons fail to develop in *Hb9* mutants (Arber et al., 1999). Cell-extrinsic cues such as the reception of input from other neurons, or of growth factors, could affect the division or survival of given target neuron or progenitor populations (see Edlund and Jessell, 1999).

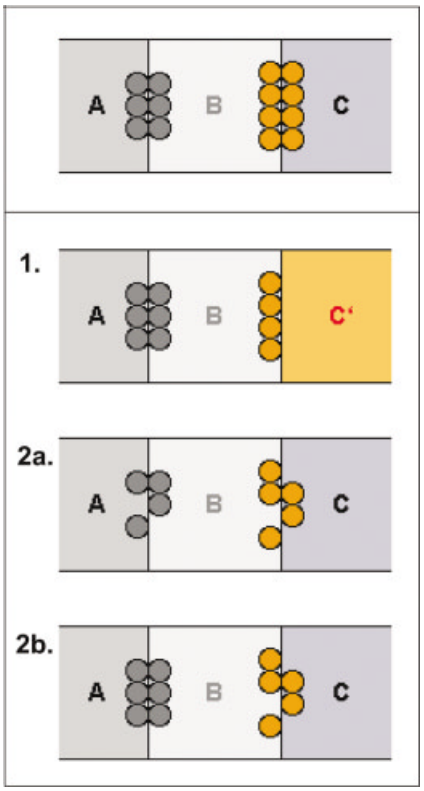

Fig. 1. Possible models for the regulation of neuronal cluster size. Two clusters are represented (dark grey and orange circles) that develop at the intersection of A and B, or B and C, patterning identities (color coded; top panel). Model 1 depicts mechanisms where the size of a cluster depends on neural tube patterning. Thus, if identity C is transformed into C′, orange neurons still develop at the B/C′ interface but their number is affected. Models 2a and b represent mechanisms controlling neuronal cluster size in a manner independent of neural tube patterning (identities A, B, and C are unchanged). In 2a, the process affected controls neuron number in all clusters (e.g., lateral inhibition). In 2b, the process affected acts locally and controls the number of orange neurons only. (Color figure can be viewed in the online issue, which is available at www.interscience.wiley.com.)

It remains unclear which combination of these models is involved in controlling the sites and extent of neurogenesis within the early anterior neural plate. To address this question, we have focused on the development of the nMLF and nPC in the embryo of the zebrafish, *Danio rerio*. Because the nMLF and nPC neurons are partially intermingled and indistinguishable before the extension of axonal processes, we have considered the development of nMLF/nPC neurons as a whole. Twenty-four hours postfertilization (hpf) teleost embryos have a relatively simple brain organization, with a scaffold of axon tracts built from a small number of neurons (Wilson and Easter, 1991; Ross et al., 1992), facilitating the analysis of developmental abnormalities. Furthermore, in the zebrafish, the nMLF/nPC is one of the first collections of neurons in the brain to appear, free of influence by other neurons. This spatial and temporal isolation from other cells undergoing similar changes also facilitates an analysis of the cues controlling nMLF/nPC development. The ontogeny of the nMLF/nPC has been precisely mapped. AChE activity or immunocytochemistry against HNK1 or acetylated-tubulin revealed the first nMLF cell bodies around 16 hr postfertilization (hpf), at the junction of the fore- (*pax6.1*-positive; Krauss et al., 1991; Püschel et al., 1992) and midbrain (*eng*-positive; Ekker et al., 1992) patterning systems along the AP axis, and along the dorsal and ventral edges of *shh* and *nkx2.2* expression, respectively, along the DV axis (Macdonald et al., 1994; Barth and Wilson, 1995; Hjorth and Key, 2001). nPC cell bodies are detectable from 18 hpf onward. They are partially intermingled with the nMLF as well as in an adjacent, more alar location in the caudal forebrain. Thus, precise molecular markers are available to assess the influence of both AP and DV cues

on neural tube patterning and nMLF/nPC development.

We report here that the transcription factor Six3, in addition to its known expression in the eye (Kobayashi et al., 1998), is specifically expressed in nMLF/nPC cell bodies from 18 hpf in the zebrafish embryo. By using *six3* expression as a marker, we then analyzed nMLF/nPC development in mutant lines affected in brain patterning (*no isthmus, smoothened/slow muscle omitted*) or in signaling from non-neural tissues (*bonnie and clyde, casanova*). Our results highlight the influence of positional cues commonly necessary for the regulation of neural tube patterning in the fore/mid area and the generation of a normal number of *six3*-positive cells. Thus, model 1 (Fig. 1) mechanisms participate in nMLF/nPC development. Surprisingly, however, we also demonstrate that a negative influence, primarily originating from the prechordal plate, is involved (directly or indirectly) in restricting the number of *six3*-positive neurons at the fore/mid border, without correlatively affecting AP or DV patterning in a detectable manner in this area. Thus, our results also demonstrate the use of cell-extrinsic signals and a type 2b mechanism to control neuronal cluster size in the anterior neural plate.

RESULTS

six3 Is Coexpressed With *GATA 3* (*gta3*) and Is an Early Marker of nMLF/nPC Neurons

nMLF and nPC neurons are identifiable at 30 hpf by their HNK-1 immunoreactivity (Fig. 2A–C, brown staining). The nMLF/nPC neurons are organized as two longitudinal branches, which are merged at their caudal end; nMLF neurons form the ventral branch (brown arrow in Fig. 2B), whereas nPC neurons organize along the fore/mid junction and form the dorsal branch (red arrow in Fig. 2B). During development, nMLF neurons are first detectable at 16 hpf (15 somites) by HNK1 staining (Fig. 2E, brown staining), whereas nPC neurons become visible at 18 hpf (not shown).

To determine whether both neuronal groups share developmental properties, we conducted an in situ hybridization search for mRNA markers jointly identifying these two neuronal populations between 16 and 36 hpf. *gta3* expression was reported in a population of HNK1-positive neurons in the ventral di- and mesencephalon from 20 hpf onward (Neave et al., 1995), where it was interpreted to label nMLF neurons before their differentiation. *six3* expression was also described in the ventral midbrain from 24 hpf onward (Kobayashi et al., 1998). We found that *gta3* expression is initiated in that location as early as 17 hpf (16–18 somites; not shown) and *six3* expression at 18 hpf (18 somites), immediately after the onset of HNK1 immunoreactivity (Fig. 2E–H, blue staining). Like *gta3, six3* expression defines a cluster comprising HNK1-positive cells in the nMLF and nPC (Fig. 2G,H, and data not shown). At 26 hpf, *six3* expression organizes as two branches, of which the ventral branch encompasses the nMLF and the dorsal branch represents the nPC (Fig. 2A–C, blue staining and arrows). At all stages, *six3* expression appears in exact overlap with *gta3*-positive cells (Fig. 2D). *six3*-positive cells are located away from the ventricular surface (black arrow in Fig. 2G), suggesting that they correspond to postmitotic neurons. A similar observation was made for *gta3* expression (Neave et al., 1995). Because cells positive for *six3* but negative for HNK1 are generally located in a more ventricular location than doubly positive cells (see Fig. 2C,G), *six3* expression might identify nMLF/nPC neurons from an earlier differentiation state than HNK1 immunoreactivity.

The location of the nMLF has been mapped relative to the expression of several molecular markers in the 24 hpf zebrafish brain (Macdonald et al., 1994; Barth and Wilson, 1995; Hauptmann and Gerster, 2000; Hjorth and Key, 2001). It lies at the interface of *shh* and *nkx2.2* expression, overlapping the caudal boundary of *pax6.1* expression. To further characterize this region molecularly, we positioned *six3* expression relative to a series of additional territorial and neuronal markers at 26 hpf, when it defines the nMLF/nPC domain (Fig. 2I–P). Along the dorsoventral axis, we found that *six3* expression straddles the *nkx2.2*-positive band (Fig. 2J). Along the AP axis, it is entirely located anterior to the mesencephalic expression domain of Eng proteins (Fig. 2K), and its dorsal branch crosses the *pax6.1* expression border (Fig. 2I). Its caudal-most cells coexpress *hoxa1a* and lie immediately adjacent to the *bts1*-positive nucleus of the basal mesencephalon (Fig. 2O,P; McClintock et al., 2001; Shih et al., 2001; Tallafuß et al., 2001). Finally, *six3* expression partially overlaps markers delimiting territories undergoing neurogenesis, such as *zcoe2, zash1a,* and *zash1b* (Fig. 2L–N; Allende and Weinberg, 1994; Bally-Cuif et al., 1998). Results are summarized in Figure 2Q.

nMLF and nPC neurons arise in neighboring locations, however, nPC neurons develop with a few hours delay, and exhibit a distinct projection pattern (nMLF axons project posteriorly, nPC axons project dorsally). Our identification of *gta3* and *six3* expression as distinctly identifying both neuronal populations suggests that the formation of these two clusters responds to shared developmental processes. We next studied which mechanisms condition the proper development of the nMLF/nPC cluster. Because *six3* only labels the nMLF/nPC region at the fore/mid AP level (in contrast to *gta3,* also expressed in underlying structures), we focused on this marker for subsequent analyses.

six3 Expression Depends on Proper Patterning of Territories Adjacent at the Fore/Mid Border

We first wished to test the involvement of neural tube patterning on the positioning and size of nMLF/nPC neurons. To this aim, we studied *six3* expression in patterning mutants where one of the territorial identities normally adjacent to the *six3* cluster is altered, albeit without tissue deletion (similar to Fig. 1, model 1).

pax2.1/noi^{tu29a} mutants fail to maintain the midbrain–hindbrain boundary organizer and lack mid-

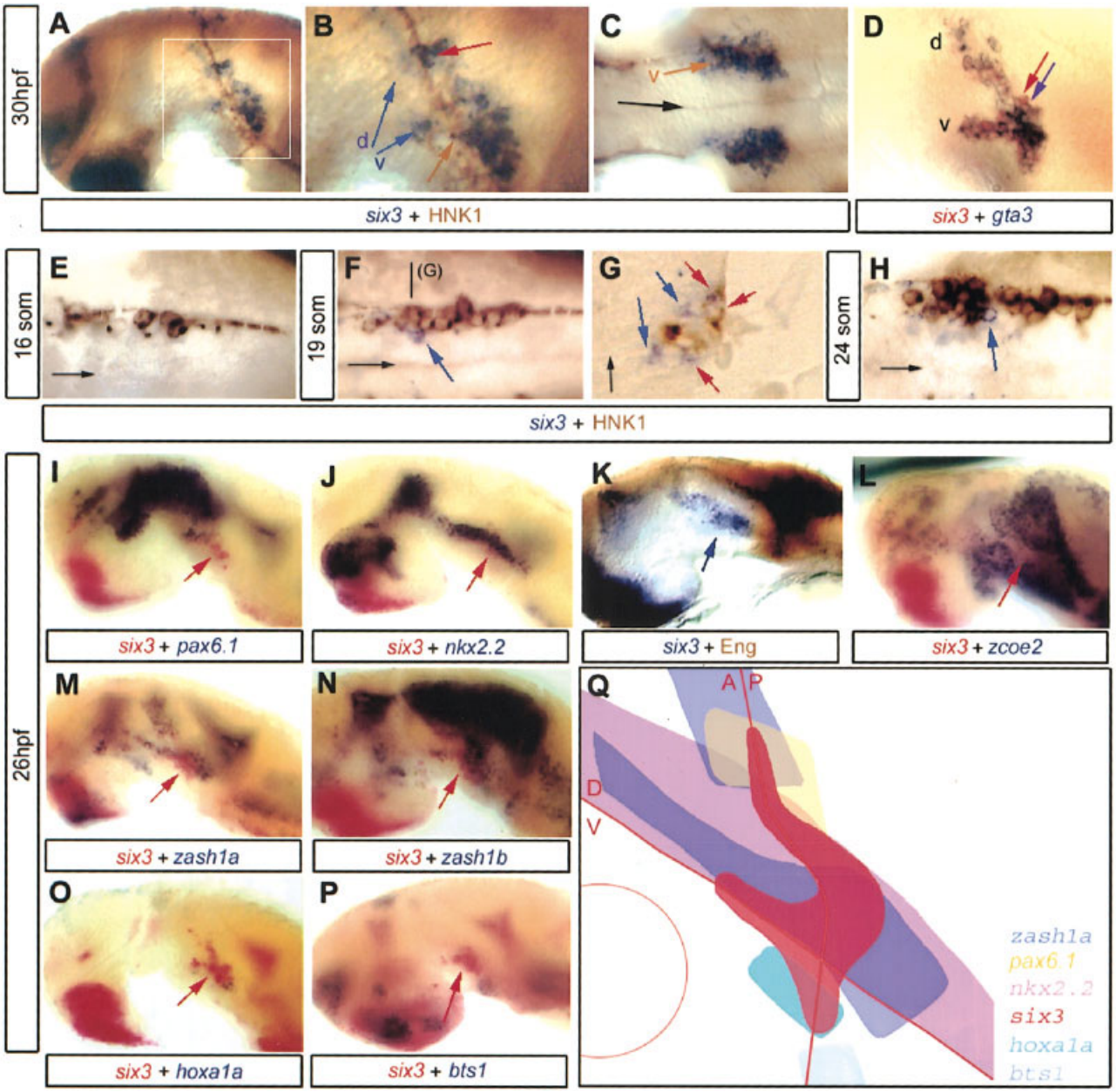

Fig. 2. *six3* expression at the forebrain/midbrain border identifies the medial longitudinal fascicle (nMLF)/posterior commissure (nPC) population and lies at the intersection of patterning markers' expression. Whole-mount embryos were processed for in situ hybridization and/or immunocytochemistry for the markers indicated (color-coded) and flat-mounted A,B,D,I–P: Sagittal views of the head, anterior left; B: High magnification of the area boxed in A; D: View of the same domain from a 26 hours postfertilization (hpf) embryo probed for *six3* and *gta3* expression; C,E,F,H: Dorsal views of the di- and mesencephalon, focused on the basal plate, anterior left, black arrows point to the ventricular zone of the neural tube; G: Cross-section of F at the level indicated, black arrow points to the ventricular zone. **A–D:** At 26–30 hpf, *six3* expression organizes as two longitudinal branches (blue arrows in B point to the dorsal (d) and ventral (v) branches, the black arrow points to the ventral branch in C) that encompass the nMLF (brown arrow in B,C) and nPC (red arrow in B), and exactly coincide with *gta3* expression (red arrows to *six3* and blue arrows to *gta3* in D). **E–H:** *six3* expression immediately follows HNK1 immunoreactivity of the nMLF and also labels cells located immediately adjacent to the HNK1-positive cluster toward the ventricular side (blue arrows point to cells only expressing *six3* in F,G,H, red arrows point to doubly labeled cells in G). **I–P:** *six3* expression (red or blue arrows) overlaps boundaries of territorial (I–K) and neurogenesis (L–P) markers: it crosses the anteroposterior boundary of *pax6.1* expression (I) but is anterior to the midbrain Eng-positive domain (K), it overlaps the *nkx2.2* DV stripe (J) and is partially overlapping with major sites of ongoing neurogenesis defined by *zcoe2*, *zash1a*, and *zash1b* expression (L–N); the most ventrocaudal *six3*-positive cells coexpress *hoxa1a* (O) but not *bts1* (P). These findings are recapitulated at high magnification in a schematized form in **Q** (color-coded; red lines to the fore/mid (AP) and *shh/nkx2.2* (DV) boundaries, circle indicates the projection of the center of the eye). som, somite.

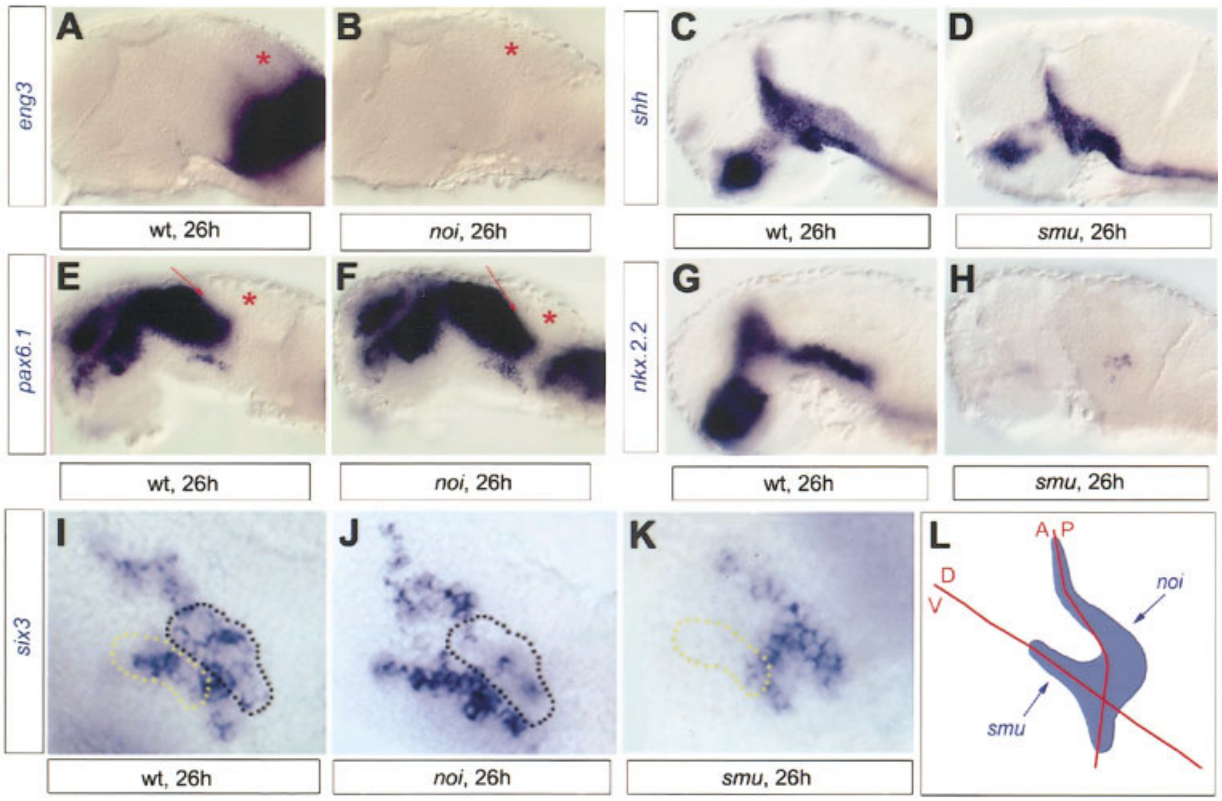

Fig. 3. Distinct subdomains of *six3* expression respond to mesencephalon and basal plate patterning deficiencies. **A–H:** Expression of the patterning markers *eng3*, *shh*, *Pax6.1*, and *nkx2.2* in *noi*^{tu29a} (B,F), *smu*^{b641} (D,H), and their wild-type (wt) siblings (A,C,E,G) at 26 hours postfertilization (h, hpf; flat-mounts of the brain, anterior left). *eng3* expression is lost in *noi*^{tu29a} (A,B), but the posterior border of *Pax6.1* expression (arrows in E,F) is unperturbed and abuts progeny cells of mesencephalic precursors (asterisks). *shh* expression is maintained in *smu*^{b641} (C,D), but the *nkx2.2*-positive identity of the territory it abuts is altered (G,H). **I–K:** Expression of *six3* at the fore/mid boundary at 26 hpf in wild-type (I), *noi*^{tu29a} (J), and *smu*^{b641} (K) mutants (high magnification of the *six3*-positive area in flat-mounted preparations, anterior left). Dotted lines surround affected domains of *six3* expression (posterior part of the dorsal branch in *noi*^{tu29a}, black dots; ventral branch in *smu*^{b641}, yellow dots). **L:** Schematic representation of the *six3*-positive cluster (blue) and the different subdomains of this cluster that are affected in *noi*^{tu29a} vs. *smu*^{b641} (blue arrows). The red lines depict the DV and AP patterning boundaries intersected by the *six3* cluster, as in Figure 2Q.

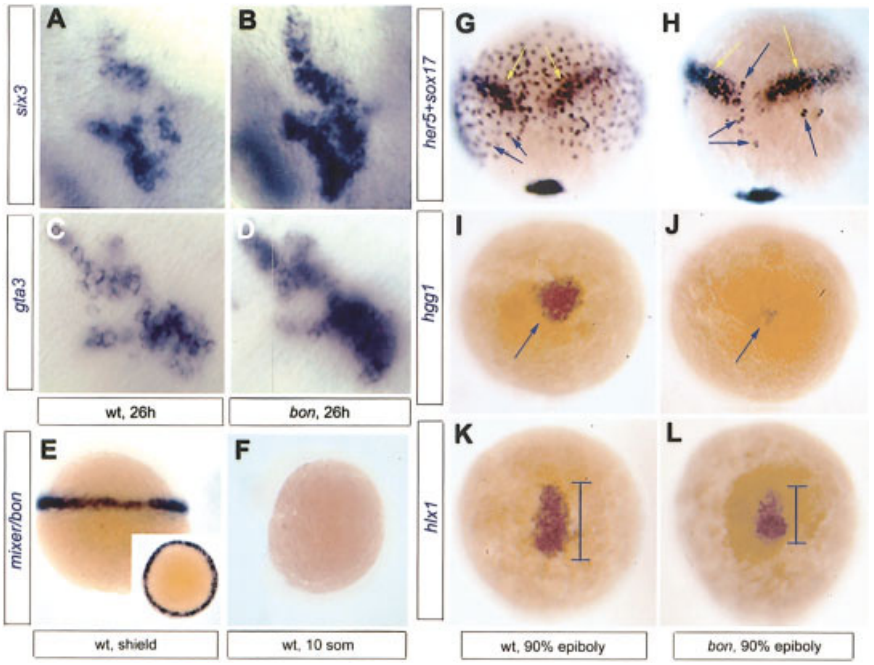

Fig. 4. The number of *six3*-positive cells in the fore/midbrain is increased in *bon* mutants, which display molecular alterations in the endoderm and prechordal plate (PCP). **A–D:** Expression of *six3* (A,B) and *gta3* (C,D) at the fore/mid boundary in 26 hours postfertilization (h) wild-type (wt; left) and *bon*^{m425} mutants (right) as indicated, anterior left. The number of *six3*- (or *gta3*-) positive cells is 1.5 times increased in *bon*^{m425}. **E,F:** Expression of *bon/mixer* in wild-type embryos, sagittal views, anterior left; inset: top view) is restricted to precursors of the endoderm, PCP and YSL at gastrulation (E) and is absent from neuroectodemal precursors at all stages (10-somite (som) stage in F). **G,H:** Expression of neural plate markers (e.g., *her5*, yellow arrows) are not affected in *bon*^{m425}, but endodermal markers (*sox17*, blue arrows) are reduced. **I–L:** Expression of the PCP markers *hgg1* (hatching gland precursors; I,J) and *hlx1* (medial pharyngeal precursors; K,L) are also reduced in *bon*^{m425} (all views dorsal, anterior up).

brain identity by 24 hpf (Lun and Brand, 1988; Brand et al., 1996). This finding is, for instance, reflected by the loss of *eng3* expression (Fig. 3A,B). However, progeny cells of midbrain precursors are still present (asterisks in Fig. 3A,B,E,F, and data not shown) and abut *pax6.1* expression (arrows in Fig. 3E,F). *noi*^{tu29a} mutants thus provide a typical example of a patterning defect where, as in model 1, a B/C interface (*pax6.1*$^{+}$,*eng3*$^{-}$/*pax6.1*$^{-}$,*eng3*$^{+}$) is replaced by B/C′ (*pax6.1*$^{+}$,*eng3*$^{-}$/*pax6.1*$^{-}$,*eng3*$^{-}$; Fig. 1, model 1). We found that the *six3* cluster still formed at the *pax6.1* border but that the caudal domain of the dorsal branch of *six3*-expression (area surrounded with black dots in Fig. 3I,J) was significantly reduced in all *noi*^{tu29a} mutants (average number of positive cells in this area: 6 ± 2 cells, n = 3 in *noi*^{tu29a} mutants compared with 36 ± 3 cells, n = 3 in wild-type siblings; Fig. 3, compare I and J).

smoothened/slow muscle omitted (*smu*^{b641}) mutants fail to transduce Hh signaling (Barresi et al., 2000; Chen et al., 2001; Varga et al., 2001), they are defective in ventral forebrain development and display strongly down-regulated *nkx2.2* expression (Varga et al., 2001; Fig. 3G,H). However, progeny of the precursors cells for the *nkx2.2*-positive domain is present, as attested by the development of motor neurons (Chen et al., 2001; Varga et al., 2001), and abuts seemingly normal *Shh* expression (Fig. 3C,D; see also Chen et al., 2001; Varga et al., 2001). Thus, *smu*^{b641} mutants can likely be considered as another example of patterning defects similar to model 1 (Fig. 1), along the DV axis. We found that fewer cells expressed *six3* in all *smu*^{b641} mutants at 26 hpf, with greatest reduction in the ventral branch (area surrounded by yellow dots in Fig. 3I,K; number of positive cells in this area: 3 ± 1 cells, n = 3 in *smu*^{b641}; 17 ± 2 cells, n = 3 in wild-type (wt)).

Together, these results support several conclusions. First, the positioning of the nMLF/nPC neuronal cluster appears to be crucially controlled by the intersection of distinct positional identities, rather than by these identities per se. Indeed, *six3* expression is induced even when some of the adjacent identities are altered. Second, the size of the nMLF/nPC neuronal cluster is sensitive to identity changes of the different territories that it contacts (Fig. 1, model 1). This sensitivity is reminiscent of the behavior of other neuronal clusters located at territorial boundaries within the embryonic brain. For instance, the nTPOC, which differentiates along the dorsal boundary of the hypothalamus, fails to form when hypothalamic identity is perturbed (Mathieu et al., 2002). Our findings also extend those of Mastick et al. (1997) reporting fewer nPC neurons in *Pax6* mouse mutants. Third, our results indicate that the response of *six3* expression to patterning defects is not all or none but is limited to the subpopulation of *six3*-positive cells overlapping or in contact with the mispatterned territory (schematized in Fig. 3L). Thus, although the nMLF/nPC cluster is characterized as a whole by *six3* expression, its size is controlled by neural tube patterning in a modular manner.

Number of *six3*-Expressing Cells at the Fore/Mid Border Depends on the Function of *bonnie and clyde/mixer*

In contrast to the phenotypes described above, all characterized by a decreased number of *six3*-positive cells, we found that the *six3*-positive cluster was significantly enlarged in the mutant *bonnie and clyde/mixer* (*bon*^{m425}; Kikuchi et al., 2000) from 24 hpf onward (80 ± 5 cells in wt, n = 30; 130 ± 6 cells in *bon* at 26 hpf, n = 30; Fig. 4A,B). The overall shape of the *six3* cluster was maintained, indicating no anisotropy in the increase in cell number along the AP or DV axes. Similar observations were made looking at *gta3* expression (Fig. 4C,D), demonstrating that the phenotype observed reflects an alteration in the size of the neuronal cluster rather than the specific upregulation of *six3* expression. To determine whether this phenotype reflected a general mispatterning of the fore/mid area, we probed *bon* embryos at 90% epiboly, 15 and 24 hpf for patterning and neurogenesis markers, including the combination described above (Fig. 2I–P). None of these profiles showed any detectable size alteration in the fore/mid area at any stage (see *her5* expression in Figure 4G,H, yellow arrows, and data not shown). Thus, we conclude that Bon/Mixer function is selectively involved in limiting the number of *six3*-positive cells in the fore/mid territory in vivo.

The primary phenotype of *bon* mutants is the near complete absence of endodermal precursors and derivatives (Kikuchi et al., 2000). Second, *bon* mutants suffer from cardia bifida and exhibit collapsed brain ventricles. To date, however, no brain patterning or neurogenesis defects have been reported in *bon*. *bon/mixer* encodes a homeodomain protein, the expression of which is restricted to the blastoderm margin, including the yolk syncytial layer (YSL), at early gastrulation (Alexander et al., 1999; Aoki et al., 2002; and see Fig. 4E). These domains are fated to the endoderm proper (gut), the prechordal plate (PCP, which later will give rise to the hatching gland and the medial part of the pharynx) and the YSL (see Fig. 5A, colored domains). The early expression of *bon/mixer* does not encompass neuroectodermal precursors (Woo and Fraser, 1995; Varga et al., 1999, Warga and Nüsslein-Volhard, 1999), and no *bon/mixer* expression is detected in the neural plate until at least 36 hpf (Fig. 4F, and data not shown). Thus, increased *six3*-positive cell number in *bon* must secondarily result from the lack of *bon/mixer* expression in precursors of the endoderm, PCP, and/or YSL.

To identify the origin of the *six3* phenotype in *bon*, we first determined which of the endodermal, PCP, and/or YSL cell populations were primarily defective in these mutants. *bon* mutants lack most endodermal precursors (Kikuchi et al., 2000; Aoki et al., 2002; see Fig. 4G,H), but a requirement for Bon/Mixer alone in PCP or YSL development was not documented (Poulain and Lepage, 2002). We found that *bon* mutants also exhibit reduced PCP and PCP derivatives such as the hatching gland, identified respectively by *hlx1* and *hgg1* expression at late gastrulation stages (Fig. 4I–L; average of 130 ± 15 *hlx1*-positive cells

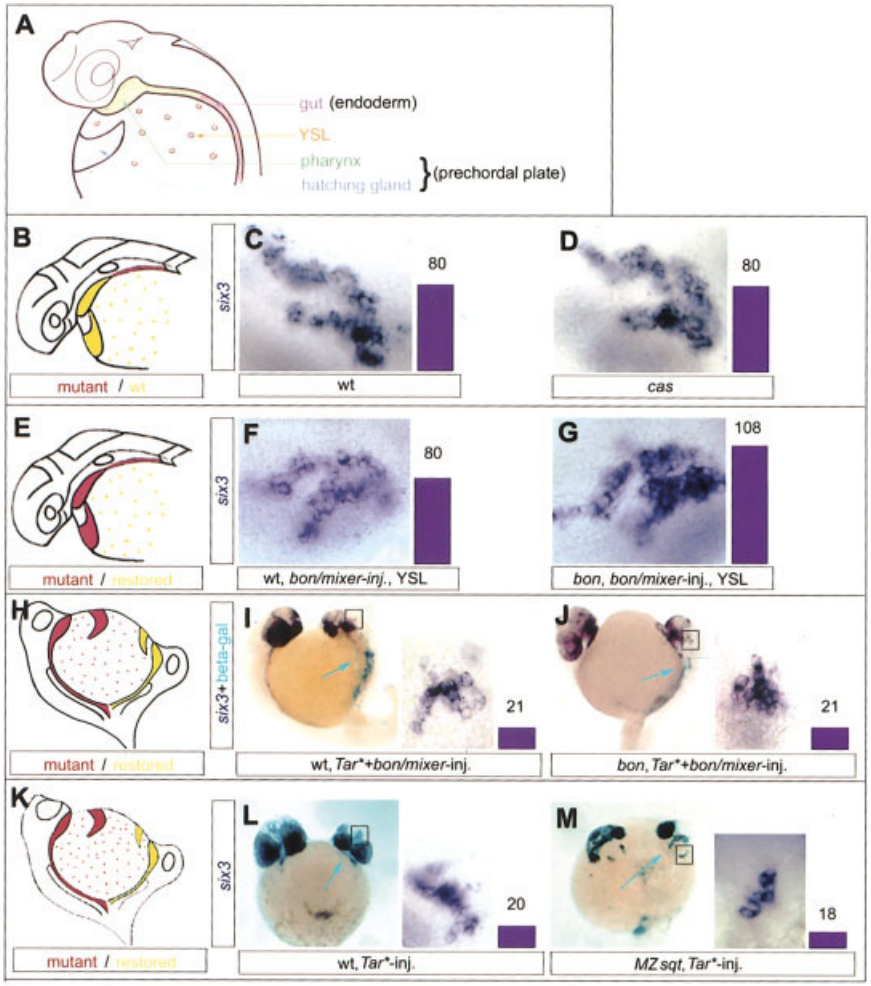

Fig. 5.

Fig. 5. The prechordal plate (PCP), but not by means of Nodal signaling, is responsible for the *six3* phenotype in *bon* mutants. **A:** Schematic localization and nomenclature for the derivatives of the domains expressing *bon/mixer* at gastrulation (color-coded). Blue, hatching gland; green, medial aspect of the pharynx (blue and green derivatives together originate from the PCP); purple, gut (derives from the endoderm proper); orange, yolk syncytial layer (YSL). **B–D:** Altered endoderm in *bon* does not alone cause the *six3* phenotype. B: Schematics of the non-neural structures that are mutant (endoderm, red) and wild-type (wt; PCP derivatives and YSL, yellow) in *casanova* (*cas*). C,D: High magnifications of the *six3*-positive cluster and corresponding cell counts (purple bars), are identical between wild-type (C) and cas^{ta56} mutant siblings (D). **E–G:** Lack of Bon/Mixer function in the YSL does not alone account for the *six3* phenotype. E: Schematics of the non-neural structures that remain mutant (endoderm and PCP, red) and are rescued (YSL, yellow) in bon^{m425} upon injection of capped *bon/mixer* mRNA into the YSL. F,G: High magnifications of the *six3*-positive cluster, and corresponding cell counts, reveal the maintenance of a mutant *six3* phenotype upon YSL rescue in bon^{m425}. **H–J:** Altered PCP causes the *six3* phenotype in *bon*. H: Schematics of the non-neural structures that remain mutant (endogenous axis: endoderm, PCP, and YSL, red) and are rescued (duplicated axis: endoderm and PCP, yellow) in bon^{m425} upon co-injection of capped *Tar*+bon/mix* mRNAs into one marginal blastomere at the 16-cell stage. I,J: Injected embryos, high magnifications of the *six3*-positive cluster of the secondary axes, and corresponding cell counts, show identical number of *six3*-positive cells upon PCP rescue in bon^{m425}. **K–M:** The PCP signal deficient in *bon* and causing the *six3* phenotype is not the Nodal factor Sqt. K: Schematics of the structures that remain mutant (endogenous axis: endoderm, PCP and YSL, red) and are rescued, except for their production of Sqt (duplicated axis: endoderm and PCP, yellow) in *MZsqt* mutants upon injection of capped *Tar** mRNA into one marginal blastomere at the 16-cell stage. L,M: Injected embryos, high magnifications of the *six3*-positive cluster of the secondary axes, and corresponding cell counts, show no significant difference in the number of *six3*-positive cells upon PCP rescue in *MZsqt*.

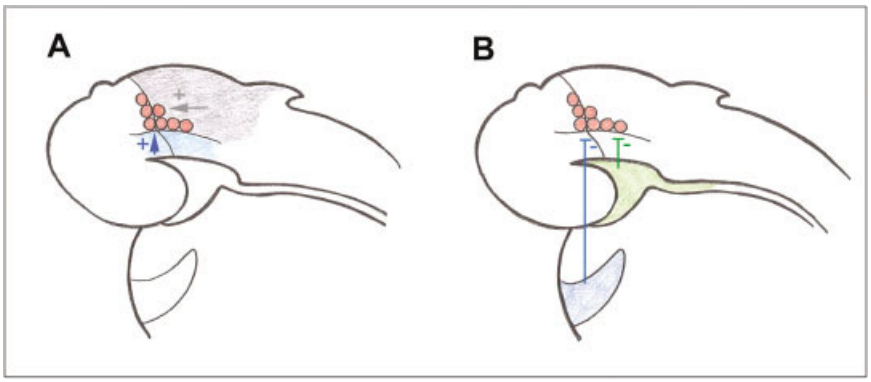

Fig. 6. Combined mechanisms integrate at the fore/mid boundary to control the size of the *six3*-positive cluster (red). **A:** Mesencephalic (grey) and basal (blue) identities positively control (arrows) the number of *six3*-positive cells that develop within these domains. **B:** The prechordal plate or its derivatives (blue, green) negatively control at a distance (bars) the overall number of *six3*-positive cells at the fore/mid boundary, without influencing neural tube patterning in this area.

in 77% of *bon* mutants, n = 8 (other *bon* mutants showed wild-type *hlx1* expression), vs. 220 ± 20 cells in wild-type, n = 21; average of 12 ± 2 *hgg1*-positive cells in 100% of *bon* mutants, n = 6, vs. 150 ± 10 cells in wild-type, n = 14). It is unlikely that this phenotype results from the lack of endoderm in *bon*: indeed, *casanova* (*cas*) mutants, which like *bon* lack endodermal precursors, have a normal PCP (Alexander et al., 1999). Thus, the defective PCP in *bon* likely reflects a direct role of Bon/Mixer in PCP precursors.

We next addressed whether *bon* mutants displayed abnormal YSL.

We found that *bon* embryos do form a morphologic YSL, visible at the dome stage by microscopic inspection (not shown). Because the function and expression profile of the YSL have not been determined; however, one cannot exclude that the YSL is not fully functional in *bon*. Thus, we conclude that the *six3* phenotype in *bon* might be caused by primary defects in the endoderm, PCP, and/or YSL. To determine which of these tissues accounts for the *six3* phenotype, we undertook selective rescue experiments to dissect the relative role(s) of each structure (endoderm, PCP, and YSL) in the generation of the *six3* expression defect.

Altered *six3* Expression in *bon* Results From a Defective Prechordal Plate

We first determined whether the *six3* phenotype in *bon* was due to the lack of endodermal precursors or derivatives. To this aim, we monitored *six3* expression in *cas* mutants. *cas* is selectively deficient in endoderm (Fig. 5B, red) but has normal PCP and YSL (Fig. 5B, yellow; Alexander et al., 1999; Dickmeis et al., 2001; Kikuchi et al., 2001; Sakaguchi et al., 2001). Patterning of the anterior neural plate in *cas* appeared normal at all stages (not shown), suggesting that endodermal factors are generally dispensable for brain development in zebrafish. In addition, we found no difference in the number of fore/mid *six3*-positive cells between *cas* and wild-type embryos at 26 hpf (80 $\pm$ 5 cells in *cas* embryos, n = 7, against 80 $\pm$ 5 cells in wild-type siblings, n = 23; Fig. 5C,D). Thus, the lack of endoderm alone can be excluded as causing the *six3* phenotype in *bon*.

Next, to address whether the *six3* phenotype was due to the lack of Bon/Mixer expression in the YSL, we selectively rescued Bon/Mixer function in this layer (Fig. 5E, yellow, vs. endoderm and PCP, red). Capped mRNA encoding Bon/Mixer (20 pg) was injected into the YSL at the 1,000-cell stage (n > 100). Co-injected *lacZ* RNA controlled for the distribution of the injected product throughout the YSL, and embryos showing uneven distribution of beta-galactosidase were discarded. We observed that injected *bon* mutants displayed a reduced cardiac phenotype compared with their noninjected mutant siblings: they developed a heart in medial position, identifiable by morphology and expression of the heart field marker *gata6* (not shown). However, this heart was much smaller than wild-type, indicative of poor rescue. In contrast, injections of *bon/mixer* into the blastoderm of one-celled embryos fully rescued the endoderm deficiency and cardia bifida phenotypes (not shown). These results suggest that the rescue of Bon/Mixer function in the YSL can only partially compensate for the lack Bon/Mixer activity overall. In addition, we found that *bon* embryos that had selectively inherited *bon/mixer* RNA into the YSL showed a *six3* phenotype comparable to that of uninjected *bon* mutants (108 $\pm$ 3 cells in the fore/mid *six3*-positive cluster in injected *bon* at 26 hpf, n = 15, vs. 80 $\pm$ 5 cells in injected wild-types, n = 15; Fig. 5F,G). Thus, the lack of Bon/Mixer activity in the YSL alone is not sufficient to account for the *six3* phenotype in *bon*.

To test the involvement of the PCP in generating the *six3* phenotype in *bon*, we rescued this tissue (together with the endoderm) in *bon* by making use of the constitutively active form of the TGFβ type I receptor Taram-A (Tar*). Tar* drives its expressing cells toward endodermal and PCP fates (Peyrieras et al., 1998; David and Rosa, 2001). When injected into one marginal blastomere at the 16-cell stage, *Tar** mRNA induces the formation of a secondary axis in which the entire endoderm and PCP, and exclusively these structures, derive from the injected cell (see Bally-Cuif et al., 2000; Aoki et al., 2002; David et al., 2002; Mathieu et al., 2002). Thus, to rescue Bon/Mixer function in the PCP (and endoderm), we co-injected *Tar** and *bon/mixer* mRNAs into a *bon* embryo. Then, *Tar** induces a secondary axis where Bon/Mixer function is selectively rescued in the endoderm and PCP (Fig. 5H, yellow). At 26 hpf, injected *bon* mutant embryos could be identified by prominent cardia bifida in their unrescued endogenous axis (Fig. 5H, red), whereas their secondary axis no longer displayed a morphologic *bon* phenotype. We thus compared the number of fore/mid *six3*-positive cells in the secondary axes of injected *bon* mutants and their injected wild-type siblings. Only embryos displaying a complete secondary axis (i.e., with anterior head and eyes) were considered. We found a comparable number of fore/mid *six3*-positive cells in the secondary axes of both injected mutants and injected wild-types (21 $\pm$ 1 cells in *bon*, n = 19, vs. 21 $\pm$ 1 cells in wild-type, n = 21; Fig. 5I,J). Thus, rescuing Bon/Mixer function in the endoderm and PCP of *bon* mutants is sufficient to rescue their *six3* phenotype. Because the lack of endoderm alone does not result in a *six3* phenotype (see above *cas* mutants), we conclude that the increased number of fore/mid *six3*-positive cells in *bon* results from deficient PCP development. Thus, the PCP selectively controls, from a distance, the size of the *six3* cluster, supporting an involvement for model 2b (Fig. 1) in the development of the nMLF/nPC cluster.

PCP Factor Controlling the Number of Fore/Mid *six3*-Positive Cells Is not a Nodal Signal

Bon/Mixer encodes a transcription factor and, thus, is unlikely to be the direct mediator of PCP activity in its regulation of *six3* expression. Several signaling factors originate from the PCP. Among those, Nodal signals have received most attention and are involved in forebrain induction and patterning in zebrafish (Rohr et al., 2001; Mathieu et al., 2002, and references therein). We thus tested whether deficient Nodal signaling from the impaired PCP in *bon* could influence the number of fore/mid *six3*-positive cells. To this aim, we studied *six3* expression in embryos where Nodal signaling from the PCP, or the reception of Nodal signals by the neural tube, is impaired.

Maternal-zygotic (MZ) *squint* (*MZsqt*), *cyclops* (*cyc*), and *MZ one-eyed pinhead* (*MZoep*) mutants are compromised in Nodal signaling. *sqt* and *cyc* encode Nodal proteins,

and *oep* is a coreceptor for Nodal factors (Feldman et al., 1998; Rebagliati et al., 1998; Sampath et al., 1998; Gristman et al., 1999; Zhang et al., 1998). Because induction of the endoderm and PCP directly requires the reception of maternal Nodal signals, *MZsqt*, *cyc*, and *MZoep* embryos fail to form all or part of these tissues. Tar* can activate the Nodal pathway downstream of the reception of Nodal signals. Thus, the injection of *Tar** into a marginal cell of 16-celled *MZsqt*, *cyc*, and *MZoep* mutant embryos restores the formation of the endoderm and PCP. The rescued axial structures of injected *MZsqt* and *cyc* mutants are still deficient in their production of a Sqt or Cyc Nodal signal, respectively, whereas the neuroectoderm of injected *MZoep* mutants is deficient in its processing of Nodal signaling. We thus used these properties to study *six3* expression in conditions where the PCP is present but produces less Nodal signal (Tar*-injected *MZsqt* or *cyc*) and in conditions where the PCP is producing Nodal normally but the overlying neuroectoderm cannot process these signals (Tar*-injected *MZoep*). As above, only embryos displaying a full secondary axis were considered. Injected mutant embryos were identified by the prominent cyclopia of their unrescued endogenous axis (Fig. 5K, red), while their secondary axis was rescued in this phenotype (Fig. 5K, yellow). We found no significant difference in the number of fore/mid *six3*-positive cells between the induced axes of wild-type (20 $\pm$ 1 cells, n = 12), *MZsqt* (18 $\pm$ 1 cells, n = 6; Fig. 4L,M), *cyc* and *MZoep* embryos (n = 3, not shown). We conclude that the PCP factor limiting the number of fore/mid *six3*-positive cells in vivo is unlikely to be a Nodal signal.

DISCUSSION

Our results demonstrate that nMLF/nPC neurons, which develop at the intersection of AP and DV patterning cues, are uniquely identified by their common expression of the transcription factor Six3 (or Gta3). This provides molecular support to the idea that neuronal clusters developing at territorial boundaries display unique molecular identities. We further show that *six3* expression is still induced at patterning borders in *noi* and *smu* mutants, where patterning is altered. These findings support the view that the positioning of early neuronal clusters is triggered by the interaction of distinct identities, rather than by these identities themselves. Finally, we used the unique *six3* molecular signature to address which mechanism(s) (Fig. 1) control the size of the nMLF/nPC in vivo. As expected, and as previously demonstrated for other neuronal clusters or for the nMLF/nPC in other species (Barth and Wilson, 1995; Mastick et al., 1997; Mathieu et al., 2002), we showed that the size of the *six3* domain is reduced when its neighboring patterning cues are altered, supporting a role for model 1 (Fig. 1) in the control of cluster size within the anterior neural plate. Surprisingly, however, we observed that the alterations of *six3* cluster size in response to patterning are not homogeneous. Rather, they primarily affect the subpopulation of *six3*-positive cells normally lying within or adjacent to the mispatterned area. Thus, *six3* expression responds to patterning influences in a modular manner. These results support a model where the control of neuronal cluster size by patterning cues is complex and involves a combination of general information (encoded by patterning boundaries) and local cues (encoded by the patterning identities themselves). Finally, our findings also highlight for the first time the existence of an inhibitory influence that selectively limits the number of *six3*-positive neurons at the fore/mid boundary, without affecting neural plate patterning, in agreement with model 2b (Fig. 1). We further demonstrate that this influence originates from the PCP. Together our findings unravel some of the combined mechanisms that control nMLF/nPC cluster size (Fig. 6A,B).

The PCP is remarkable for its influence on forebrain patterning, permitting the development of ventral di- and telencephalic structures at the expense of dorsal identities. Our results provide the first report of (direct or indirect) activity of the PCP on more posterior brain domains. The requirement for Bon/Mixer in PCP cells alone must take place at an early stage, because *bon/mixer* expression is switched off from the blastoderm margin immediately after the shield stage. However, the exact timing of PCP activity that influences the *six3* cluster cannot be determined from our experiments. The PCP and at least some of its derivatives (such as the medial aspect of the pharynx) underlie the presumptive midbrain/diencephalic area at all gastrulation and somitogenesis stages. This leaves ample time for the PCP to influence the number of *six3*-positive cells at the fore/mid boundary.

The mechanism controlling *six3* cluster size that is impaired in *bon* remains currently unclear. We did not observe specific cell death in the fore/mid area in wild-type embryos at any stage (acridine orange and TUNEL assays, not shown). Likewise, we failed to detect differences in cell proliferation between wild-type and *bon* mutants in this area (anti-phosphohistone H3 immunocytochemistry, not shown). Thus, an influence of the PCP on cell death or cell proliferation in the fore/mid area can likely be excluded. It follows that the increased number of *six3*-positive cells in *bon* rather resembles a neurogenic phenotype, i.e., the development of more neurons than normal due to the production of a higher number of neuronal progenitors. However, because of its selectivity, it appears unlikely to involve a general neurogenesis process, e.g., lateral inhibition, which would be expected to affect all or most neuronal clusters (Fig. 1, model 2a). Growth of the *six3*-positive cluster appeared similarly progressive over time in wild-type and *bon* embryos, and a significant difference in cell number between *bon* embryos and their wild-type siblings only appeared at 26 hpf. In several instances, neuronal differentiation was shown to occur in successive waves, which drive entry into terminal mitoses in a spatiotemporally regulated manner (Hu and Easter, 1999; Kay et al., 2001). Thus, it is possible that the abnormally numerous *six3* cells in *bon* result from either an earlier entry into a phase of terminal

divisions by some *six3* precursors, or a greater bias for some of these precursors to leave the cell cycle, which might prematurely induce a differentiation wave and be detectable around the 26 hpf stage using our molecular markers.

Because the *six3* phenotype in *bon* is not accompanied by mispatterning of the fore/mid brain area, our observations provide an example for model 2b (Fig. 1), where a (direct or indirect) non–cell-autonomous influence selectively acts on the size of one neuronal cluster. Other examples where the size of a specific early neuronal population is regulated by external signals without influence on local patterning, as well as without involving local events of cell proliferation or death, are scarce. One reported case is the retina, where differentiation appears also controlled by PCP-derived signals in the zebrafish (Masai et al., 2000): *ath5* is a marker of differentiating retinal neurons, it is selectively absent in *oep* mutants without correlative defects on retinal identity, and it is rescued in *oep* embryos injected with *Tar**. In this case, the signaling and relay process involved were identified: nodal signaling from the PCP promotes the production of Shh by optic stalk tissue, which in turn regulates retinal *ath5* expression (Masai et al., 2000). Within the brain proper, one case of such a mechanism was also reported recently: the control of the number of catecholaminergic and serotonergic neurons in the zebrafish hypothalamus by the zinc finger transcription factor Too few/Fezl (Levkowitz et al., 2003). This process is non–cell-autonomous and does not affect forebrain patterning (Levkowitz et al., 2003). The regulation of *six3* cluster size that we unravel here, thus, provides a second example of such a mechanism during primary neurogenesis within the brain proper. The influence of the PCP demonstrated here is also unique in that it is involved in limiting rather than increasing the number of *six3*-positive neurons at the fore/mid boundary. In both cases, for Too few/Fezl and monoaminergic neurons, or for the PCP and *six3*, the relay mechanisms and factors involved remain unknown. Our data suggest that Nodal signaling alone from the PCP can be excluded as a regulator of *six3* cluster size. However, the PCP expresses several other signaling factors that, alone or in combination, could account for *six3* regulation. For example, BMP4, BMP7 and ADMP, Shh and Twhh, Wnts, and opponent secreted factors such as Dkk, are expressed in the PCP at gastrulation or later stages. The selective role of these factors in mediating PCP development or function remains, with a few exceptions, unexplored. Understanding which combination of PCP factors is involved in the selective control of *six3* expression will require partial functional rescue of the PCP in *bon* by the coinjection of *Tar** and the relevant morpholinos or dominant-negative mutant forms.

EXPERIMENTAL PROCEDURES

Fish Strains

Embryos were obtained from natural spawning of AB or the following mutant lines: *bon*^{m425} (Kikuchi et al., 2000), *cas*^{ta56} (Chen et al., 1996), *cyc*^{b16} (Hatta et al., 1991), *sqt*^{cz35} (Heisenberg and Nüsslein-Volhard, 1997), *noi*^{tu29a} (Brand et al., 1996), *ace*^{ti282a} (Brand et al., 1996), and *smu*^{b641} (Barresi et al., 2000). Heterozygous adult carriers were intercrossed to obtain mutant embryos. *MZsqt* embryos, deficient in both the maternal and zygotic contributions of the *sqt* locus, were obtained by raising weakly affected *sqt* homozygous embryos to adulthood. The resulting homozygous *sqt* adults were then intercrossed. All embryos were raised and staged according to Kimmel et al. (1995).

Rescue Experiments

To rescue endo- and mesendodermal tissues in the duplicated axes of Nodal mutant embryos (e.g., *MZsqt*), capped *Taram-A** (*Tar**) mRNA (8 pg; Peyrieras et al., 1998) was injected into one marginal blastomere of 16-celled embryos. For similar rescues in *bon*^{m425}, because Mixer acts at least in part downstream of Tar* activity, capped *bon/mixer* mRNA (20 pg) was co-injected with *Tar**. All experiments were lineage-traced by coinjecting *nls-lacZ* mRNA (60 pg). To rescue the function of Bon/Mixer in the YSL of *bon* mutant embryos, capped *bon/mixer* mRNA (20 pg) was injected into the morphologically visible YSL in 1,000-celled embryos, together with *nls-lacZ* mRNA as lineage tracer.

In the case of *Tar** injections leading to the formation of a fully duplicated axis at 26 hpf, *bon* and *MZsqt* mutant embryos were identified by the characteristic mutant phenotype maintained by their endogenous axis. In all other experiments, to identify *bon* mutant embryos after injection, in situ hybridization and/or cell counts, embryos were a posteriori genotyped by polymerase chain reaction as described in Kikuchi et al. (2000).

Staining for Marker Expression

In situ hybridization and immunocytochemistry were carried out according to standard protocols (Thisse et al., 1993; Hauptmann and Gerster, 1994; Bally-Cuif and Wassef, 1994). The following probes and antibodies were used: *bon/mixer* (Kikuchi et al., 2000), *bts1* (Tallafuβ et al., 2001), *gta3* (Neave et al., 1995), *her5* (Müller et al., 1996), *hgg1* (Thisse et al., 1994), *hlx1* (Seo et al., 1999), *hoxa1a* (McClintock et al., 2001), *nkx2.2* (Barth and Wilson, 1995), *pax6.1* (Nornes et al., 1998), *six3* (Seo et al., 1998), *sox17* (Alexander and Stainier, 1999), *zash1a* and *zash1b* (Allende and Weinberg, 1994), *zcoe2* (Bally-Cuif et al., 1998), anti-infected 4D9 antibody (recognizing all zebrafish Eng proteins; DHSB; dilution 1/8), and anti-HNK1 (DHSB zn12; dilution 1/500). X-Gal staining was performed by incubation in 4 mM Kferrocyanide, 4 mM Kferricyanide, 4 mM $MgCl_2$, 400 ng/μl Xgal in phosphate buffered saline, after 25 min fixation in 2% paraformaldehyde; 0.2% glutaraldehyde at room temperature. Flat-mounted embryos were photographed and scored under a Zeiss Axioplan microscope.

Cell Counts

To estimate the number of cells positive for *six3* (or *gta3*) expression, flat-mounted preparations of in situ hy-

bridization–stained embryos were observed under ×20 or ×40 magnification and Nomarski optics to visualize nuclei. Each nucleus that appeared fully surrounded by a ring of stained cytoplasm was counted. Repeated blind counts on each specimen were carried out, and the modal value (i.e., the most frequent count for a given specimen analyzed several times) for each specimen was determined. The modal value never differed of more than 5% from the extreme counts. Results are expressed here, for each experiment, as the average of the modal values between specimens, ± the standard deviation.

ACKNOWLEDGMENTS

We thank A. Folchert and B. Tannhäuser, who provided expert technical assistance throughout this work. We also thank Drs. J. Mathieu and N. Peyrieras for *sqt* adult homozygotes, F. Rosa for *MZoep* embryos, D. Stainier for the *bon/mixer* line, and numerous colleagues for probes and reagents. We thank current lab members, members of the K. Imai group, and Drs. S. Easter, L. Puelles, F. Rosa, D. Stainier, and M. Wassef for discussions at different stages of this work; and Drs. S. Easter, G. Mastick, and J. Favor for their critical reading of the manuscript. The monoclonal antibodies zn12 developed by B. Trevarrow and 4D9 were obtained from the Developmental Studies Hybridoma Bank maintained by the University of Iowa, Department of Biological Sciences, Iowa City, IA 52242. L.B-C.'s laboratory was funded by the VolkswagenStiftung Association and DFG.

REFERENCES

Alexander J, Stanier DY. 1999. A molecular pathway leading to endoderm formation in zebrafish. Curr Biol 9:1147–1157.

Alexander J, Rothenberg M, Henry GL, Stainier DYR. 1999. Casanova plays an early and essential role in endoderm formation in zebrafish. Dev Biol 215:343–357.

Allende ML, Weinberg ES. 1994. The expression pattern of two zebrafish achate-scute homolog (ash) genes is altered in the embryonic brain of the Cyclops mutant. Dev Biol 166:509–530.

Aoki TO, David NB, Minchiotti G, Saint-Etienne L, Dickmeis T, Persico GM, Strähle U, Mourrain P, Rosa FM. 2002. Molecular integration of Casanova in the Nodal signaling pathway controlling endoderm formation. Development 129:275–286.

Arber S, Han B, Mendelsohn M, Smith M, Jessell TM, Sockanathan S. 1999. Requirement for the homeobox gene Hb9 in the consolidation of motor neuron identity. Neuron 23:659–674.

Ba-Charvet KT, von Boxberg Y, Guazzi S, Boncinelli E, Godement P. 1998. A potential role for the OTX2 homeoprotein in creating early "highways" for axon extension in the rostral brain. Development 125:4273–4282.

Bally-Cuif L, Wassef M. 1994. Ectopic induction and reorganization of *Wnt-1* expression in quail/chick chimeras. Development 120:3379–3384.

Bally-Cuif L, Dubois L, Vincent A. 1998. Molecular cloning of *Zcoe2*, the zebrafish homolog of *Xenopus Xcoe2* and mouse *EBF-2*, and its expression during primary neurogenesis. Mech Dev 77:85–90.

Bally-Cuif L, Goutel C, Wassef M, Wurst W, Rosa F. 2000. Coregulation of anterior and posterior mesendodermal development by a hairy-related transcriptional repressor. Genes Dev 14:1664–1677.

Barresi MJ, Stickney HL, Devoto SH. 2000. The zebrafish slow-muscle-omitted gene product is required for Hedgehog signal transduction and the development of slow muscle identity. Development 127:189–199.

Barth KA, Wilson SW. 1995. Expression of zebrafish nk2.2 is influenced by sonic hedgehog/vertebrate hedgehog-1 and demarcates a zone of neuronal differentiation in the embryonic forebrain. Development 121:1755–1768.

Bertuzzi S, Hindges R, Mui SH, O'Leary DDM, Lemke G. 1999. The homeodomain protein Vax1 is required for axon guidance and major tract formation in the developing forebrain. Genes Dev 13:3092–3105.

Blader P, Strähle U. 2000. Zebrafish developmental genetics and central nervous system development. Hum Mol Genet 9:945–951.

Brand M, Heisenberg CP, Jiang YJ, Beuchle D, Lun K, Furutani-Seiki M, Granato M, Haffter P, Hammerschmidt M, Kane DA, Kelsh RN, Mullins MC, Odenthal J, van Eeden FJ, Nusslein-Volhard C. 1996. Mutations in zebrafish genes affecting the formation of the boundary between midbrain and hindbrain. Development 123:179–190.

Chédotal A, Pourquié O, Sotelo C. 1995. Initial tract formation in the brain of the chick embryo: selective expression of the BEN/SC1/DM-GRASP cell adhesion molecule. Eur J Neurosci 7:198–212.

Chen JN, Haffter P, Odenthal J, Vogelsang E, Brand M, van Eeden EJ, Furutani-Seiki M, Granato M, Hammerschmidt M, Heisenberg CP, Jiang YJ, Kane DA, Kelsh RN, Mullins MC, Nusslein-Volhard C. 1996. Mutations affecting the cardiovascular system and other internal organs in zebrafish. Development 123:293–302.

Chen W, Burgess S, Hopkins N. 2001. Analysis of the zebrafish smoothened mutant reveals conserved and divergent functions of hedgehog activity. Development 128:2385–2396.

Chitnis AB. 1999. Control of neurogenesis: lessons from frogs, fish and flies. Curr Opin Neurobiol 9:18–25.

David N, Rosa FM. 2001. Cell autonomous commitment to an endodermal fate and behaviour by activation of Nodal signaling. Development 128:3937–3947.

David N, Saint-Etienne L, Tsan M, Schilling TF, Rosa FM. 2002. Requirement for endoderm and Fgf3 in ventral head skeleton formation. Development 129: 4455–4468.

Dickmeis T, Mourrain P, Saint-Etienne L, Fischer N, Aanstadt P, Clark M, Strähle U, Rosa F. 2001. Casanova, a gene crucial for endoderm development, encodes a novel sox-related molecule. Genes Dev 15:1487–1492.

Easter SS Jr. 1994. Initial tract formation in the vertebrate brain. Prog Brain Res 102: 79–93.

Easter SS Jr, Ross LS, Frankfurter A. 1993. Initial tract formation in the mouse brain. J Neurosci 13:285–299.

Edlund T, Jessell TM. 1999. Progression from extrinsic to intrinsic signaling in cell fate specification: a view from the nervous system. Cell 96:211–224.

Ekker M, Wegner J, Akimenko MA, Westerfield M. 1992. Coordinate embryonic expression of three zebrafish engrailed genes. Development 116:1001–1010.

Feldman B, Gates MA, Egan ES, Dougan ST, Rennebeck G, Sirotkin HI, Schier AF, Talbot WS. 1998. Zebrafish organizer development and germ-layer formation require nodal-related signals. Nature 395:181–185.

Gristman K, Zhang J, Cheng S, Heckscher E, Talbot WS, Schier AF. 1999. The EGF-CFC protein one-eyed pinhead is essential for nodal signaling. Cell 97:121–132.

Hallonet M, Hollemann T, Pieler T, Gruss P. 1999. Vax1, a novel homeobox-containing gene, directs development of the basal forebrain and visual system. Genes Dev 13:3106–3114.

Hatta K, Kimmel CB, Ho RK, Walker C. 1991. The Cyclops mutation blocks specification of the floor plate of the zebrafish central nervous system. Nature 350:339–341.

Hauptmann G, Gerster T. 1994. Two-color whole-mount in situ hybridization to vertebrate and Drosophila embryos. Trends Genet 10:266.

Hauptmann G, Gerster T. 2000. Regulatory gene expression patterns reveal transverse and longitudinal subdivisions of the embryonic zebrafish forebrain. Mech Dev 91:105–118.

Heisenberg CP, Nusslein-Volhard C. 1997. The function of silverblick in the positioning of the eye anlage in the zebrafish embryo. Dev Biol 184:85–94.

Hjorth JT, Key B. 2001. Are pioneer axons guided by regulatory gene expression

domains in the zebrafish forebrain? High-resolution analysis of the patterning of the zebrafish brain during axon tract formation. Dev Biol 229:271–286.
Hu M, Easter SS Jr. 1999. Retinal neurogenesis: the formation of the initial central patch of postmitotic cells. Dev Biol 207:309–321.
Kay JN, Finger-Baier KC, Roeser T, Staub W, Baier H. 2001. Retinal ganglion cell genesis requires lakritz, a Zebrafish atonal Homolog. Neuron 30:725–736.
Kikuchi Y, Trinh LA, Reiter JF, Alexander J, Yelon D, Stainier DYR. 2000. The zebrafish bonnie and clyde gene encodes a mix family homeodomain protein that regulates the generation of endodermal precursors. Genes Dev 14: 1279–1289.
Kikuchi Y, Agathon A, Alexander J, Thisse C, Waldron S, Yelon D, Thisse B, Stainier DYR. 2001. Casanova encodes a novel Sox-related protein necessary and sufficient for early endoderm formation in zebrafish. Genes Dev 14:1279–1289.
Kimmel CB. 1993. Patterning the brain of the zebrafish embryo. Annu Rev Neurosci 16:707–732.
Kimmel CB, Ballard WW, Kimmel SR, Ullmann B, Schilling TF. 1995. Stages of embryonic development of the zebrafish. Dev Dyn 203:253–310.
Kobayashi M, Toyama R, Takeda H, Dawid IB, Kawakami K. 1998. Overexpression of the forebrain-specific homeobox gene six3 induces rostral forebrain enlargement in zebrafish. Development 125:2973–2982.
Krauss S, Johansen T, Korzh V, Moens U, Ericson JU, Fjose A. 1991. Zebrafish pax(zf-a): a paired box-containing gene expressed in the neural tube. EMBO J 10:3609–3619.
Levkowitz G, Zeller J, Sirotkin HI, French D, Schilbach S, Hashimoto H, Hibi M, Talbot WS, Rosenthal A. 2003. Zinc finger protein too few controls the development of monoaminergic neurons. Nat Neurosci 6:28–33.
Lewis J. 1998. Notch signaling and the control of cell fate choices in vertebrates. Semin Cell Dev Biol 9:583–589.
Lun K, Brand M. 1988. A series of no isthmus (noi) alleles of the zebrafish pax2.1 gene reveals multiple signaling events in development of the midbrain-hindbrain boundary. Development 125: 3049–3062.
Macdonald R, Xu Q, Barth KA, Mikkola I, Holder N, Fjose A, Krauss S, Wilson SW. 1994. Regulatory gene expression boundaries demarcate sites of neuronal differentiation in the embryonic zebrafish forebrain. Neuron 13:1039–1053.
Macdonald R, Scholes J, Strähle U, Brennan C, Holder N, Brand M, Wilson SW. 1997. The pax protein Noi is required for commissural pathway formation in the rostral forebrain. Development 124: 2397–2408.
Masai I, Stemple DL, Okamoto H, Wilson SW. 2000. Midline signals regulate retinal neurogenesis in zebrafish. Neuron 27:251–263.
Mastick GS, Easter SS Jr. 1996. Initial organization of neurons and tracts in the embryonic mouse fore- and midbrain. Dev Biol 173:79–94.
Mastick GS, Davis NM, Andrews GL, Easter SS Jr. 1997. Pax-6 functions in boundary formation and axon guidance in the embryonic mouse forebrain. Development 124:1985–1997.
Mathieu J, Barth A, Rosa FM, Wilson SW, Peyrieras N. 2002. Distinct and cooperative roles for Nodal and Hedgehog signals during hypothalamic development. Development 129:3055–3065.
McClintock JM, Carlson R, Mann DM, Prince VE. 2001. Consequences of Hox gene duplication in the vertebrates: an investigation of the zebrafish Hox paralogue group 1 genes. Development 128: 2471–2484.
Müller M, Weizsäcker Ev, Campos-Ortega JA. 1996. Transcription of a zebrafish gene of the hairy-Enhancer of split family delineates the midbrain anlage in the neural plate. Dev Genes Evol 206: 153–160.
Neave B, Rodaway A, Wilson SW, Patient R, Holder N. 1995. Expression of zebrafish GATA 3 (gta3) during gastrulation and neurolation suggests a role in the specification of cell fate. Mech Dev 51:169–182.
Nornes S, Clarkson M, Mikkola I, Pedersen M, Bardsley A, Martinez JP, Krauss S, Johansen T. 1998. Zebrafish contains two pax6 genes involved in eye development. Mech Dev 77:185–196.
Peyrieras N, Strähle U, Rosa F. 1998. Conversion of zebrafish blastomeres to an endodermal fate by TGF-β-related signaling. Curr Biol 8:783–786.
Poulain M, Lepage T. 2002. Mezzo, a paired-like homeobox protein is an immediate target of Nodal signalling and regulates endoderm specification in zebrafish. Development 129:4901–4914.
Püschel AW, Gruss P, Westerfield M. 1992. Sequence and expression pattern of pax-6 are highly conserved between zebrafish and mice. Development 114: 643–651.
Rebagliati MR, Toyama R, Haffter P, Dawid IB. 1998. Cyclops encodes a nodal-related factor involved in midline signaling. Proc Natl Acad Sci U S A 95: 9932–9937.
Rohr KB, Barth KA, Varga ZM, Wilson SW. 2001. The nodal pathway acts upstream of hedgehog signaling to specify ventral telencephalic identity. Neuron 29:341–351.
Ross LS, Parrett T, Easter SS Jr. 1992. Axonogenesis and morphogenesis in the embryonic zebrafish brain. J Neurosci 12:467–482.
Sakaguchi T, Kuroiwa A, Takeda H. 2001. A novel sox gene, 226D7, acts downstream of Nodal signaling to specify endoderm precursors in zebrafish. Mech Dev 107:25–35.
Sampath K, Rubinstein AL, Cheng AM, Liang JO, Fekany K, Solnica-Krezel L, Korzh V, Halpern ME, Wright CV. 1998. Induction of the zebrafish ventral brain and floorplate requires cyclops/nodal signalling. Nature 395:185–189.
Seo HC, Drivenes, Ellingsen S, Fjose A. 1998. Expression of two zebrafish homologues of the murine Six3 gene demarcates the initial eye primordia. Mech Dev 73:45–57.
Seo HC, Nilsen F, Fjose A. 1999. Three structurally and functionally conserved Hlx genes in zebrafish. Biochim Biophys Acta 1489:323–335.
Shih LJ, Tsay HJ, Lin SC, Hwang SP. 2001. Expression of zebrafish Hoxa1a in neuronal cells of the midbrain and anterior hindbrain. Mech Dev 101:279–281.
Tallafuß A, Wilm TP, Crozatier M, Pfeffer P, Wassef M, Bally-Cuif L. 2001. The zebrafish buttonhead-like factor Bts1 is an early regulator of pax2.1 expression during mid-hindbrain development. Development 128:4021–4034.
Thisse C, Thisse B, Schilling TF, Postlethwait JH. 1993. Structure of the zebrafish snail1 gene and its expression in wild-type, spadetail and no tail mutant embryos. Development 119:1203–1215.
Thisse C, Thisse B, Halpern ME, Postlethwait JH. 1994. Goosecoid expression in neurectoderm and mesendoderm is disrupted in zebrafish cyclops gastrulas. Dev Biol 164:420–429.
Varga ZM, Wegner J, Westerfield M. 1999. Anterior movement of ventral diencephalic precursors separates the primordial eye field in the neural plate and requires Cyclops. Development 126: 5533–5546.
Varga ZM, Amores A, Lewis KE, Yan YL, Postlethwait JH, Eisen JS, Westerfield M. 2001. Zebrafish smoothened functions in ventral neural tube specification and axon tract formation. Development 128: 3497–3509.
Warga RM, Nüsslein-Volhard C. 1999. Origin and development of the zebrafish endoderm. Development 126:827–838.
Wilson SW, Easter SS Jr. 1991. A pioneering growth cone in the embryonic zebrafish brain. Proc Natl Acad Sci U S A 88:2293–2296.
Wilson SW, Ross LS, Parrett T, Easter SS Jr. 1990. The development of a simple scaffold of axon tracts in the brain of the embryonic zebrafish Brachydanio rerio. Development 108:121–145.
Wilson SW, Placzek M, Furley AJ. 1993. Border disputes: do boundaries play a role in growth-cone guidance? Trends Neurosci 16:316–323.
Wilson SW, Brennan C, Macdonald R, Brand M, Holder N. 1997. Analysis of axon tract formation in the zebrafish brain: the role of territories of gene expression and their boundaries. Cell Tissue Res 290:189–186.
Woo K, Fraser SE. 1995. Order and coherence in the fate map of the zebrafish nervoussystem. Development 121:2595–2609.
Zhang J, Talbot WS, Schier AF. 1998. Positional cloning identifies zebrafish one-eyed pinhead as a permissive EGF-related ligand required during gastrulation. Cell 92:241–251.